Original Article

J Adv Med Biomed Res. 2024; 32(155): 405-414

Investigation of the Produced Positrons and Their Dose Deposition at Bone and Soft Tissue Organs at Proton Therapy: A Simulation Study

Amir Reza Khoshhal [1*], Ahmad Esmaili Torshabi [1*], Sharareh Babamohammadi [1]

1. *Faculty of Sciences and Modern Technologies, Graduate University of Advanced Technology, Kerman, Iran*

Article Info

10.22034/jambr.32.155.405

Received: 2024/10/09;
Accepted: 2025/01/05;
Published Online: 2025/02/28;

Corresponding Information:
Ahmad Esmaili Torshabi,
Faculty of Sciences and Modern Technologies, Graduate University of Advanced Technology, Kerman, Iran
E-Mail:
ahmad4958@gmail.com
Amir Reza Khoshhal,
Faculty of Sciences and Modern Technologies, Graduate University of Advanced Technology, Kerman, Iran
E-Mail:
amirrezakhoshhal79@gmail.com

ABSTRACT

Background & Objective: Proton therapy has emerged as a superior method in cancer treatment compared to traditional photon-based radiation therapies. Because of the unique physical features of protons and Bragg curve, it can deliver the greatest dosage directly to the tumor while minimizing the radiation absorbed by surrounding healthy tissues. By spreading out Bragg Peak, proton therapy ensures that the tumor receives the prescribed high dose while reducing side effects. In proton therapy, the positrons play a significant role in dose monitoring and imaging.

Materials & Methods: In this research, GEometry ANd Tracking (GEANT4) simulation code was used to study the number of positrons emitted and their dose depositions during proton therapy at energies of 50 and 100 MeV in both soft tissue and bone with variety of densities.

Results: The results showed that for 50 MeV protons, ^{15}O was identified as the positron emitter that emits the most positrons in both tissues at two energies. The maximum penetration depth of 50 MeV proton beam was 26 mm in soft tissue and 16 mm in bone, while at 100 MeV, the depth was 89 mm in soft tissue and 53 mm in bone. Furthermore, the dose deposition by positrons decreases by increasing tissue density.

Conclusion: In proton therapy 50 and 100 MeV the most positrons emitted from ^{15}O, ^{11}C, ^{30}P, ^{13}N, ^{38}k, ^{39}Ca in soft tissue and bone. Bragg curves show that by increasing energy, the rate of proton penetration in tissues increases. On the other hand, by increasing density, the amount of proton penetration in tissues and dose deposition decreases.

Keywords: Proton therapy, Positron emitters, Dose deposition, GEANT4 simulation code

Copyright © 2023, This is an original open-access article distributed under the terms of the Creative Commons Attribution-noncommercial 4.0 International License which permits copy and redistribution of the material just in noncommercial usages with proper citation.

Introduction

Recent studies showed that the side effects resulting from cancer treatment, such as secondary cancers, cardiovascular diseases, and other long-term effects, manifest years after the initial cancer therapy (1-7). Today, achieving cancer treatment with fewer side effects is considered a major milestone (8). Proton therapy, a type of radiotherapy, is recognized as one of the methods for cancer treatment, capable of treating various types of cancer by precisely targeting the tumor while minimizing damage to surrounding healthy tissues (9). The proton beam's dosage distribution curve is its main benefit. Because of this curvature, the tumor may be completely destroyed without endangering the healthy tissues around it. Proton therapy is one of the best ways to treat cancer because of this characteristic, which also lowers adverse effects and improves treatment effectiveness (10). A high-energy proton beam moves toward the target tissue (such as a tumor). As protons pass through the tissue, they interact with nuclei present in the tissue (such as 12C and 16O). These interactions produce radioactive isotopes like 11C, 13N, and 15O, which are positron-emitting isotopes. These radioactive isotopes undergo decay over a short period, emitting positrons. The positrons rapidly collide with electrons, initiating the annihilation process, which results in producing two gamma photons of 511 keV in opposite directions. These photons are detected by detectors, providing precise imaging of dose distribution. In 1946, Robert Wilson introduced proton therapy as a novel method for treating

deep-seated tumors using high-energy protons produced by accelerators to destroy cancer cells (11). In 1962, Harvard University began specialized treatment using proton therapy at the Cyclotron Laboratory (12, 13). By mid-1970s, with the advancement of radiotherapy studies, various organs, such as the eyes and ears were studied using this method (14). Bragg peak, which occurs at the end of the range of charged particles like protons, is a significant advantage. However, high dose decrease at the end of the spectrum might cause an increase in dosage to healthy tissues with even a little shift in particle location. Thus, careful monitoring and control of charged particle dosage distribution are required to determine their range. It shows that despite the inherent advantages of charged particles, careful control and management of treatment parameters are necessary in this method (15). GEANT 4 is a Monte Carlo simulation tool widely used in high-energy physics research, medical physics, accelerator design, and other related fields. It enables accurate modeling of particle passage via matter and their interactions. Using Geant, phenomena, such as scattering, absorption, particle production, and nuclear reactions can be simulated (16, 17). Mashayekhi M. et al., conducted a simulation of a phantom to evaluate the relationship between the production of positron emitters and proton dose distribution, as well as the correlation between annihilation points, and proton dose distribution. The findings indicated that 15O, 11C and 13N are the most appropriate positron emitters in soft tissue, while 11C, 15O, 38K, 30P, 39Ca, and 13N are the most suitable in bone tissue (18). In other study, Kraan A.C. et al., simulated a proton therapy treatment course for a patient using FLUKA Monte Carlo simulations. The progressive emptying of the sinonasal cavity was represented by constructing a series of artificially manipulated CT images (19). In this work, the number of released positrons in entire and meshed target volume of target and the dosage deposited of positrons during proton treatment at energies of 50 and 100 MeV in soft tissue and bone with variety of densities were explored. The results obtained using GEANT 4 code. The highest number of positrons was produced by 15O. It should be noted that the highest number of positrons being produced at a depth of 60-70 mm in soft tissue and 30-40 mm in bone. The maximum dose deposition of positrons in soft tissue and bone occur in density of 0.9 gr/cm3 and 1.6 gr/cm3 respectively.

Materials and Methods

The research utilized GEANT4 toolkit, a Monte Carlo simulation tool that models the passage of particles through matter. GEANT4 is commonly applied in the fields, such as high-energy physics, nuclear physics, accelerator physics, as well as medical and space science, to simulate particle interactions with materials. One of its key strengths is its ability to accurately define complex geometries and material properties within experimental setups, while handling various physics processes for particle transport through detector elements. The toolkit supports simulations in a wide energy range, from one eV to 1012 eV, making it highly effective for replicating real-world experimental conditions, including physical models and geometry. This accuracy distinguishes it from other simulation packages. Because GEANT4 is designed in C++, it can simulate particle interactions with materials in great detail, down to the microscopic level. It is extensively used in fields such as high-energy physics investigations, gamma-ray shielding, and medical physics (20, 21). The physics model used in this study is QGSP_BIC_HP that is the most widely used and comprehensive physical model in Geant4 for proton therapy studies. (22) (Figure 1A) illustrates the flowchart of GEANT4 modeling (23). In this study, GEANT4 version of 11.1.3 was utilized. Furthermore, a 60-core processor with 160 GB of RAM was used.

In this study, as shown in (Figure 1B), a target volume with dimensions of 10×10×10 cm^3 was defined using GEANT4 simulation code. A 50 and 100 MeV proton beam with a 1 cm width was directed towards the target volume (Figure 1B). The source was positioned 1 cm away from the target volume. The target volume contained soft tissue with densities of 0.9, 1, and 1.1 g/cm^3, as well as bone tissue with densities of 1.6, 1.7, and 1.8 g/cm^3 based on the predefined parameters. The overall number of created positrons and the number of positrons generated from distinct positron emitters following the proton beam's contact with these tissues were estimated, and the Bragg curve was constructed. In the next step, the target volume was meshed along with one axis into 10 volumes, each with the dimensions of 10×10×1 cm^3, with no gaps in between. The proton beam was again directed towards these volumes, with a density of 0.9, 1 and 1.1 g/cm^3 for soft tissue and 1.6, 1.7 and 1.8 g/cm^3 for bone tissue (Figure 1C). In this manner, the number of positrons emitted per unit volume (100 cm^3) and at a depth of 1 cm was determined. Moreover, in the next part the absorbed dose of positrons at bone with density of 1.6, 1.7 and 1.8 g/cm^3 and soft tissue with density of 0.9, 1 and 1.1 g/cm^3 was calculated.

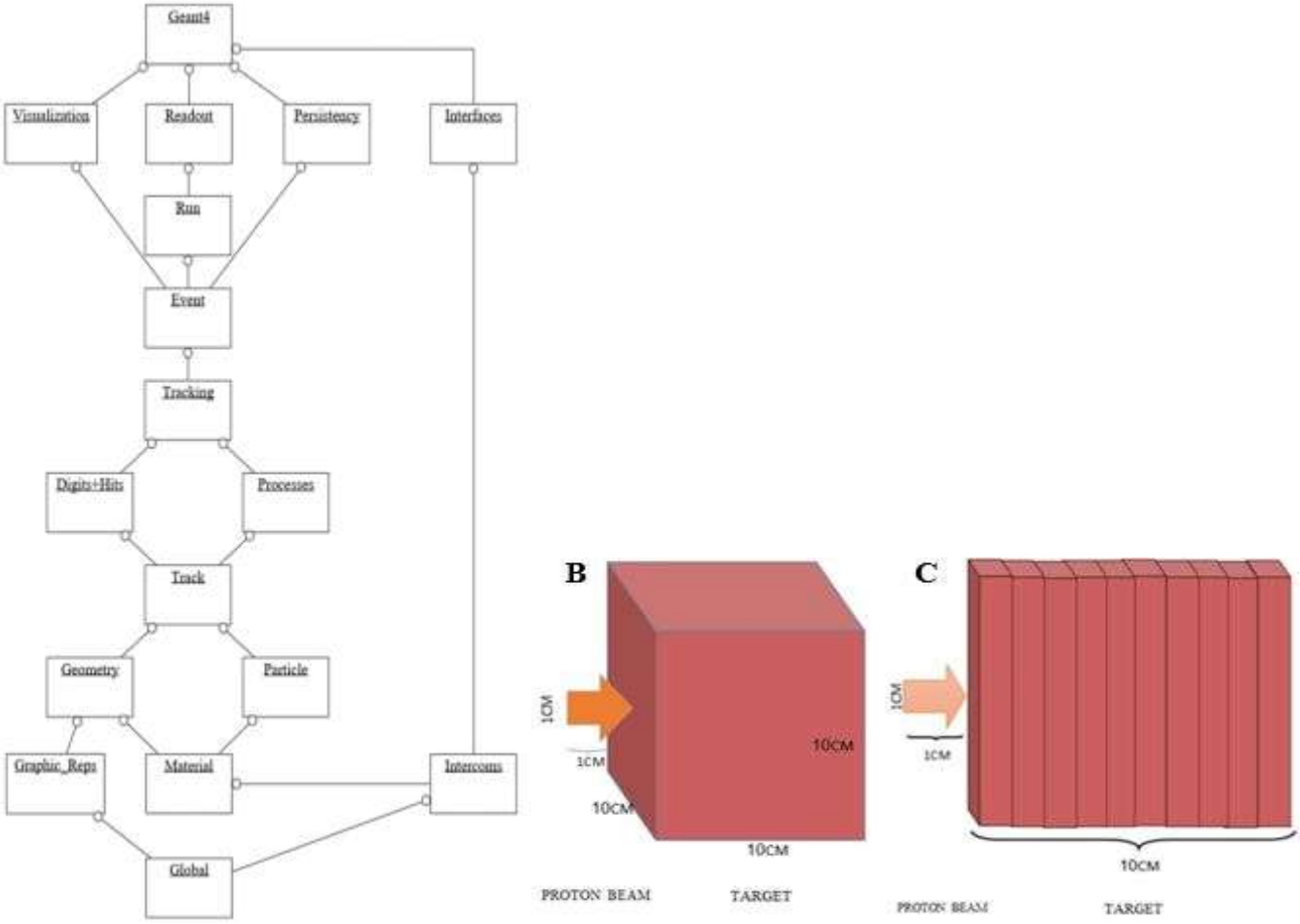


Figure 1. Flowchart of the GEANT4 modeling process (A), Schematic of proton beam irradiation to the target volume in GEANT4 (B, C).

Results

Using GEANT4 simulation code, a proton beam was directed at a target volume consisting of soft tissue and bone tissue with various densities. Different positron emitters and the number of emitted positrons by them within a 1000 cm³ volume are shown in (Table 1).

Table 1. Number of positrons emitted per unit volume (10^3 cm³) at 50 MeV (A) and 100 MeV (B)

A						
Positron emitters	**Soft tissue**			**Bone**		
	$\rho = 0.9$ gr/cm³	**$\rho = 1$ gr/cm³**	**$\rho = 1.1$ gr/cm³**	**$\rho = 1.6$ gr/cm³**	**$\rho = 1.7$ gr/cm³**	**$\rho = 1.8$ gr/cm³**
^{8}B	0.015	0.017	0.017	0.007	0.011	0.004
^{10}C	0.029	0.024	0.023	0.023	0.019	0.017
^{11}C	1.206	1.259	1.263	2.078	2.177	2.118
^{12}N	0.069	0.045	0.058	0.136	0.136	0.129

^{13}N	0.525	0.504	0.470	0.417	0.422	0.407
^{14}O	0.029	0.037	0.031	0.027	0.039	0.037
^{15}O	5.207	5.225	5.168	3.167	2.921	2.921
^{18}F	0.204	0.213	0.197	0.128	0.142	0.131
^{22}Na	-	-	-	0.010	0.008	0.010
^{23}Mg	-	-	-	0.009	0.012	0.014
^{26}Al	-	-	-	0.020	0.027	0.036
^{29}P	-	-	-	0.030	0.042	0.037
^{30}P	-	-	-	0.874	0.897	0.916
^{31}S	-	-	-	0.104	0.099	0.116
^{34}Cl	-	-	-	0.005	0.006	0.011
^{35}Ar	-	-	-	0.009	0.009	0.009
^{37}K	-	-	-	0.005	0.007	0.015
^{38}K	-	-	-	0.566	0.587	0.573
^{38}Ca	-	-	-	0.007	0.010	0.003
^{39}Ca	-	-	-	0.460	0.482	0.511
^{40}Sc	-	-	-	0.052	0.041	0.042
^{41}Sc	-	-	-	0.026	0.030	0.023
^{42}Sc	-	-	-	0.005	0.001	0.006
^{43}Sc	-	-	-	0.013	0.012	0.010
^{44}Sc	-	-	-	0.019	0.009	0.020
^{27}Si	-	-	-	0.003	0.004	0.005

B

Positron emitters	**Soft tissue**			**Bone**		
	$\rho = 0.9$ gr/cm^3	**$\rho = 1$ gr/cm^3**	**$\rho = 1.1$ gr/cm^3**	**$\rho = 1.6$ gr/cm^3**	**$\rho = 1.7$ gr/cm^3**	**$\rho = 1.8$ gr/cm^3**
^{8}B	0.194	0.181	0.177	0.155	0.119	0.135
^{10}C	0.253	0.259	0.270	0.318	0.291	0.292
^{11}C	4.072	4.160	4.169	7.150	7.043	7.099
^{12}N	0.180	0.166	0.177	0.329	0.314	0.329
^{13}N	2.268	2.247	2.186	1.621	1.580	1.610
^{14}O	0.637	0.631	0.648	0.409	0.430	0.432
^{15}O	15.598	15.614	15.487	8.858	8.750	8.879
^{18}F	0.229	0.220	0.216	0.126	0.118	0.119
^{22}Na	-	-	-	0.051	0.053	0.058
^{23}Mg	-	-	-	0.030	0.035	0.023
^{26}Al	-	-	-	0.147	0.168	0.160
^{29}P	-	-	-	0.175	0.213	0.167
^{30}P	-	-	-	1.912	1.849	1.898
^{31}S	-	-	-	0.203	0.199	0.186
^{33}Cl	-	-	-	0.036	0.031	0.035
^{34}Cl	-	-	-	0.349	0.349	0.293
^{35}Ar	-	-	-	0.048	0.056	0.065
^{37}K	-	-	-	0.191	0.190	0.168
^{38}K	-	-	-	2.129	2.211	2.132
^{38}Ca	-	-	-	0.084	0.097	0.086
^{39}Ca	-	-	-	1.442	1.426	1.351
^{40}Sc	-	-	-	0.096	0.095	0.079

^{41}Sc	-	-	-	0.028	0.027	0.030
^{42}Sc	-	-	-	0.004	0.008	0.006
^{43}Sc	-	-	-	0.019	0.015	0.017
^{44}Sc	-	-	-	0.012	0.008	0.012
^{27}Si	-	-	-	0.022	0.027	0.030

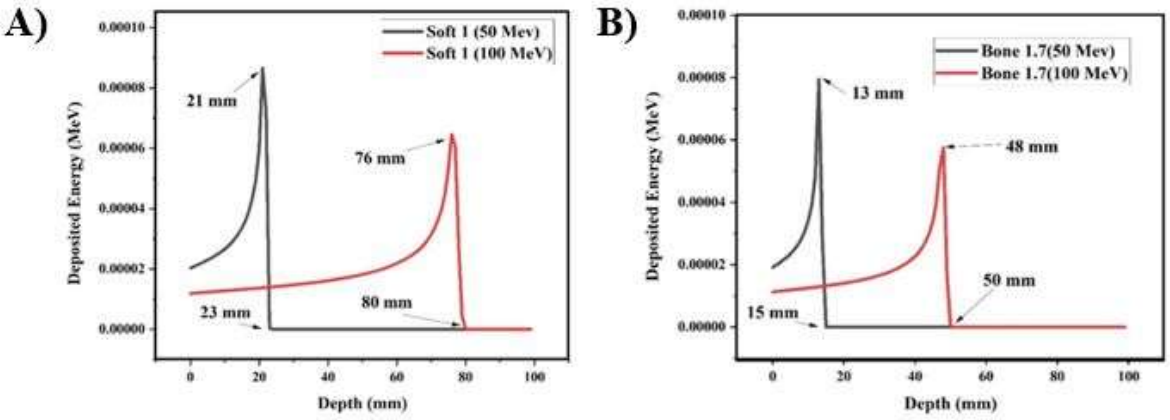


Figure 2. The Bragg curves for soft tissue with density of 1 gr/cm^3 (A) and bone with density of 1.7 gr/cm^3 (B), at two energies, 50 and 100 MeV.

In (Table 2), the depth of proton in soft tissue and bone at various density at two energies, 50 and 100 MeV was showed.

The number of positrons emitted at 1 cm intervals for two different energies presents in (Table 3).

Table 2. The Depth of proton in soft tissue and bone at various density at two energies, 50 and 100 MeV

Tissue		Soft tissue		Bone	
		$\rho = 0.9$ gr/cm^3	$\rho = 1.1$ gr/cm^3	$\rho = 1.6$ gr/cm^3	$\rho = 1.8$ gr/cm^3
Depth(mm)	50 MeV	26	21	16	14
	100 MeV	89	73	53	47

Table 3. Number of positrons emitted per unit volume at 50 MeV (A) and 100 MeV (B) (10^2 cm^3).

	A									
Tissue	0-10 mm	10-20 mm	20-30 mm	30-40 mm	40-50 mm	50-60 mm	60-70 mm	70-80 mm	80-90 mm	90-100 mm
Soft $\rho = 0.9$ gr/cm^3	38.98	31.92	3.86	0.30	0.21	0.12	0.06	0.11	0.12	0.06

	$\rho = 1$ gr/cm^3	28.22	44.01	2.78	0.29	0.22	0.11	0.09	0.10	0.08	0.02
	$\rho = 1.1$ gr/cm^3	48.61	24.95	0.90	3.20	1.40	1.70	0.07	0.14	0.08	0.10
Bone	$\rho = 1.6$ gr/cm^3	74.86	10.04	0.69	0.38	0.28	0.28	0.19	0.19	0.06	0.12
	$\rho = 1.7$ gr/cm^3	76.30	8.28	0.74	0.57	0.22	0.22	0.27	0.13	0.10	0.07
	$\rho = 1.8$ gr/cm^3	77.91	6.61	0.69	0.62	0.34	0.18	0.12	0.14	0.06	0.04

B

Tissue		**0-10 mm**	**10-20 mm**	**20-30 mm**	**30-40 mm**	**40-50 mm**	**50-60 mm**	**60-70 mm**	**70-80 mm**	**80-90 mm**	**90-100 mm**
Soft	$\rho = 0.9$ gr/cm^3	25.87	25.61	27.33	27.26	27.76	30.42	36.41	34.30	5.59	0.44
	$\rho = 1$ gr/cm^3	28.19	29.54	29.72	30.85	32.95	37.94	42.63	9.48	0.69	0.41
	$\rho = 1.1$ gr/cm^3	30.43	31.91	33.33	35.37	38.27	45.69	23.86	1.56	0.45	0.46
Bone	$\rho = 1.6$ gr/cm^3	46.58	49.46	53.80	62.41	57.08	3.77	1.18	0.92	0.54	0.43
	$\rho = 1.7$ gr/cm^3	48.80	52.46	57.06	72.37	39.17	1.90	1.32	0.88	0.75	0.68
	$\rho = 1.8$ gr/cm^3	53.23	55.01	61.43	78.82	21.50	1.70	1.08	0.99	0.76	0.39

The dose deposition per positrons in soft tissue and bone with various densities at energy of 50 and 100 MeV has shown in (Table 4).

Table 4. The dose deposition per positrons in soft tissue and bone at energy of 50 MeV (A) and 100 MeV (B)

A						
Tissue	**Soft**			**Bone**		
	$\rho = 0.9$ **gr/cm^3**	$\rho = 1$ **gr/cm^3**	$\rho = 1.1$ **gr/cm^3**	$\rho = 1.6$ **gr/cm^3**	$\rho = 1.7$ **gr/cm^3**	$\rho = 1.8$ **gr/cm^3**
Dose (nGy/Positron)	2.13×10^{-4}	1.90×10^{-4}	1.73×10^{-4}	1.43×10^{-4}	1.34×10^{-4}	1.28×10^{-4}

B						
Tissue	**Soft**			**Bone**		
	$\rho = 0.9$ **gr/cm^3**	$\rho = 1$ **gr/cm^3**	$\rho = 1.1$ **gr/cm^3**	$\rho = 1.6$ **gr/cm^3**	$\rho = 1.7$ **gr/cm^3**	$\rho = 1.8$ **gr/cm^3**
Dose (nGy/Positron)	2.19×10^{-4}	1.94×10^{-4}	1.77×10^{-4}	1.43×10^{-4}	1.33×10^{-4}	1.25×10^{-4}

Discussion

Based on Table 1, the number of positrons emitted in bone tissue is greater compared to soft tissue. In soft tissue, positron-emitting nuclei, such as ^{15}O, ^{13}N, and ^{11}C were observed, while in bone tissue, positron emitters, such as ^{15}O, ^{13}N, ^{11}C, ^{39}Ca, ^{38}K and ^{30}P emitted a significant number of positrons. The emission of other β^+emitting nuclei is insignificant. In proton treatment, 15O creates the maximum quantity of positrons since oxygen is one of the fundamental components in biological tissues (particularly in water and oxygen-containing substances). Consequently, the possibility of high-energy protons engaging with 16O nuclei is larger compared to other elements. These interactions lead to nuclear reactions that produce radioactive isotope ^{15}O. The decay of ^{15}O emits positrons, which, in terms of the relative abundance of oxygen in the body, significantly contributes to positron production in proton therapy. In the study by Mashayekhi et al., the number of positrons emitted from the positron emitters ^{15}O and ^{13}N in soft tissue is very close to that in the present study. Compared to Mashayeki's study, this study demonstrated a higher number of positrons emitted by ^{11}C. In bone tissue the number of positrons emitted from positron emitters, such as ^{11}C, ^{15}O, ^{38}K and ^{13}N so close to Mashayeki's study (18). Thus, the results of this study are very similar to other studies (24-26). Based on (figure 2) and Table 2, the penetration depth of proton beam in soft tissue is 21-26 mm, while in bone tissue it is 14-16 mm in energy of 50 MeV and 73-89 mm in soft tissue and 47-53 mm in bone in energy of 100 MeV. Because soft tissue is less dense than bone, the proton beam can penetrate it more easily. The maximal energy is deposited by the proton beam in soft tissue at a depth of 76 mm and in bone tissue at a depth of 48 mm. Bragg curves show that by increasing energy, the rate of proton penetration in tissues increases. On the other hand, by increasing density, the amount of proton penetration in tissues and dose deposition decreases. Table 3 presents the number of positrons produced at 1 cm intervals. The results show that the highest number of positrons in soft tissue occurs at the depth of 50-70 mm, while in bone tissue it is at the depth of 30-40 mm for energy of 100 MeV. Furthermore, this value for energy of 50 MeV occurs at the depth of 0-10 mm in soft tissue and bone. Calculating the residual dose from positrons in proton therapy is essential for several reasons: 1) accurately assessing the radiation dose in the tumor while protecting healthy tissues, 2) assisting in optimizing treatment parameters and enhancing precision, 3) using 511 keV photons for precise imaging of dose distribution, 4) reducing the risk of damage to sensitive tissues via dose accumulation control, and 5) evaluating treatment efficacy and the body's response to proton therapy. Since the primary therapeutic dose is delivered by protons, the dose from positrons is considered an unwanted, as it is independent of the prescribed proton dose. The determination of the dosage from positrons in the target tissue is one of the study's goals. The dosage deposition

of positrons in tissues is shown in Table 4. The findings indicate that the quantity of dose deposition reduces with increasing density. The energy of incoming beam has a significant effect on the bandwidth, peak height, range, and shape of Bragg curve. In heavy particle therapy, the precise shape of Bragg curve is crucial to determine the radiation dose in various tissues. Energy deviation can cause uneven radiation dose distribution across different tissue regions. In Monte Carlo simulations, accurate modeling of energy dispersion is essential for precise predictions of particle interactions with matter. GEANT simulation code, using QGSP_BIC_HP model, was employed to predict these interactions accurately and mitigate the effects of energy deviation. The Bragg curves in the findings section demonstrate that as energy rises, the peak height falls and the curve breadth widens. This is due to the fact that higher proton beam energy causes more penetration and energy deposition in the tissue depth, which lowers the height of the curve.

Conclusion

Proton therapy is a type of radiation therapy that was studied. Proton therapy is widely used in terms of its ability to deliver the maximum dose to the target while minimizing the dose to surrounding healthy tissues. Positron creation happens during proton treatment, and using GEANT4 simulations, the quantity of positrons produced per unit target volume with different densities of soft and bone tissues was examined. The results indicated that in soft tissue and bone, the highest number of positrons was emitted by ^{15}O, 5.207 and 3.167 at energy of 50 MeV and 15.598 and 8.879 at energy of 100 MeV respectively. Therefore, Bragg curve analysis showed that the penetration depth of a 50 MeV proton beam was 26 mm in soft tissue and 16 mm in bone. Thus, the penetration depth of a 100 MeV proton beam was 89 mm and 53 mm in soft tissue and bone respectively. The quantity of positrons generated in 1 cm thicknesses was finally examined by meshing the target volume; the greatest number of positrons were generated at a depth of 60–70 mm in soft tissue and 30–40 mm in bone. The maximum dose deposition of positrons in soft tissue and bone occur in density of 0.9 gr/cm^3 and 1.6 gr/cm^3 respectively.

Acknowledgements

The authors sincerely appreciate Ms. Farideh Homayoun Amlashi for her invaluable support and contributions to this research.

Conflict of Interest

The authors declare no conflict of interest.

Funding

This research received no external funding.

Ethics approval and consent to participate

This study was approved by the ethical committee of Graduate University of Advanced Technology, Kerman, Iran.

Authors' Contribution

Conceptualization, Amir Reza Khoshhal and Ahmad Esmaili Torshabi; methodology, Amir Reza Khoshhal; software, Amir Reza Khoshhal; validation, Ahmad Esmaili Torshabi and Amir Reza Khoshhal; investigation, Sharareh Babamohammadi and Amir Reza Khoshhal; data curation, Sharareh Babamohammadi; writing—original draft preparation, Amir Reza Khoshhal and Sharareh Babamohammadi ; writing—review and editing, Ahmad Esmaili Torshabi; supervision, Ahmad Esmaili Torshabi; project administration, Ahmad- Esmaili Torshabi and Amir Reza Khoshhal.

References

1. Wilson VC, McDonough J, Tochner Z. Proton beam irradiation in pediatric oncology: an overview. J Pediatr Hematol Oncol.2005,1;27(8):444-8. https://doi.org/10.1097/01.mph.0000174030.55485.54
PMid:16096529

2. Carver JR, Shapiro CL, Ng A, Jacobs L, Schwartz C, Virgo KS, et al. American Society of Clinical Oncology clinical evidence review on the ongoing care of adult cancer survivors: cardiac and pulmonary late effects. J Clin Oncol. 2007,1;25(25):3991-4008. https://doi.org/10.1200/JCO.2007.10.9777
PMid:17577017

3. Armstrong GT, Liu Q, Yasui Y, Neglia JP, Leisenring W, Robison LL, Mertens AC. Late mortality among 5-year survivors of childhood cancer: a summary from the Childhood Cancer Survivor Study. J Clin Oncol. 2009,10;27(14):2328-38.
https://doi.org/10.1200/JCO.2008.21.1425
PMid:19332714 PMCid:PMC2677921

4. Merchant TE. Proton beam therapy in pediatric oncology. Cancer J. 2009,1;15(4):298-305. https://doi.org/10.1097/PPO.0b013e3181b6d4b7
PMid:19672146

5. Sauvat F, Binart N, Poirot C, Sarnacki S. Preserving fertility in prepubertal children. Horm Res. 2009,1;71(Suppl. 1):82-6. https://doi.org/10.1159/000178045
PMid:19153513

6. Newhauser WD, Durante M. Assessing the risk of second malignancies after modern radiotherapy. Nat Rev Cancer. 2011,11(6):438-48.

https://doi.org/10.1038/nrc3069
PMid:21593785 PMCid:PMC4101897

7. Olch AJ. Pediatric radiotherapy planning and treatment. CRC Press; 2013, 9. https://doi.org/10.1201/b14554
PMid:23726005

8. Wolff HA, Wagner DM, Conradi LC, Hennies S, Ghadimi M, Hess CF, Christiansen H. Irradiation with protons for the individualized treatment of patients with locally advanced rectal cancer: a planning study with clinical implications. Radiother Oncol. 2012,1;102(1):30-7. https://doi.org/10.1016/j.radonc.2011.10.018
PMid:22112780

9. Gragoudas ES, Goitein M, Verhey L, Munzenreider J, Urie M, Suit H, Koehler A. Proton beam irradiation of uveal melanomas: results of 5½-year study. Arch Ophthal. 1982, 1;100(6):928-34. https://doi.org/10.1001/archopht.1982.01030030936007
PMid:6284097

10. Newhauser WD, Zhang R. The physics of proton therapy. Phys Med Biol. 2015 Mar 24;60(8):R155. https://doi.org/10.1088/0031-9155/60/8/R155
PMid:25803097 PMCid:PMC4407514

11. Wilson R. A brief history of the Harvard University cyclotrons. 2017.

12. Kjellberg RN, Koehler AM, Preston WM, Sweet WH. Stereotaxic instrument for use with the Bragg peak of a proton beam. Stereotact Funct Neurosurg. 1962;22(3-5):183-9. https://doi.org/10.1159/000104360
PMid:14033248

13. Kjellberg RN, Sweet WH, Preston WM, Koehler AM. The Bragg peak of a proton beam in intracranial therapy of tumors. Transac Am Neurol Assoc. 1962 , 1;87.

14. Gragoudas ES, Goitein M, Verhey L, Munzenreider J, Urie M, Suit H, Koehler A. Proton beam irradiation of uveal melanomas: results of 5½-year study. Arch Ophthal. 1982,1;100(6):928-34. https://doi.org/10.1001/archopht.1982.01030030936007
PMid:6284097

15. Kraft G. Tumor therapy with heavy charged particles. Prog Part Nucl Phys. 2000,1;45:S473-544. https://doi.org/10.1016/S0146-6410(00)00112-5

16. Agostinelli S, Allison J, Amako KA, Apostolakis J, Araujo H, Arce P, Asai M, et al. GEANT4-a simulation toolkit. Nuclear instruments and methods in physics research section A: Accelerators, Spectrometers, Prog Part Nucl Phys. 2003,1;506(3):250-303.

17. Collaboration GE, Agostinelli S. GEANT4-a simulation toolkit. Nucl Instrum. Meth. A. 2003;506(25):0.

18. Mashayekhi M, Mowlavi AA, Jia SB. Simulation of positron emitters for monitoring of dose distribution in proton therapy. Rep. Pract Oncol Radiother. 2017,1;22(1):52-7. https://doi.org/10.1016/j.rpor.2016.10.004
PMid:27829820 PMCid:PMC5094681

19. Kraan AC, Moglioni M, Battistoni G, Bersani D, Berti A, Carra P, Cerello P, et al. Using the gamma-index analysis for inter-fractional comparison of in-beam PET images for head-and-neck treatment monitoring in proton therapy: A Monte Carlo simulation study. Physica Medica. 2024,1;120:103329. https://doi.org/10.1016/j.ejmp.2024.103329
PMid:38492331

20. Khatibani AB, Khoshhal AR, Tochaee EB, Jamnani SR, Moghaddam HM. Physical and gamma radiation shielding features of Sm2O3/graphene nanoparticles: A comparison between experimental and simulated gamma shielding capability. Inorg Chem Commun 2024,23:112772. https://doi.org/10.1016/j.inoche.2024.112772

21. Khoshhal AR, Khatibani AB, Tirehdast Z, Shaddoust M, Nirouei M. Evaluation of experimental and simulated gamma ray shielding ability of ZnCo2O4 and ZnCo2O4/graphene nanoparticles. Optical Materials. 2024,1;156:115953. https://doi.org/10.1016/j.optmat.2024.115953

22. Bongrand, A., Busato, E., Force, P., Martin, F. and Montarou, G., 2020. Use of short-lived positron emitters for in-beam and real-time β+ range monitoring in proton therapy. Physica Medica, 2020,1;69,248-255. https://doi.org/10.1016/j.ejmp.2019.12.015
PMid:31918377

23. Khoshhal AR, Esmaili Torshabi A. Feasibility of Anthropomorphic Head Phantom Design Using DLP 3D Printing for Dosimetry. J Nucl Res Appl. 2024,21;4(3):22-33. https://doi.org/10.24200/jonra.2024.1634.1140

24. Seravalli, E., Robert, C., Bauer, J., Stichelbaut, F., Kurz, C., Smeets, J., et al, 2012. Monte Carlo calculations of positron emitter yields in proton radiotherapy. Physics in Medicine & Biology, 57(6), p.1659. https://doi.org/10.1088/0031-9155/57/6/1659 PMid:22398196

25. Pshenichnov, I., Mishustin, I. and Greiner, W., 2006. Distributions of positron-emitting nuclei in proton and carbon-ion therapy studied with GEANT4. Physics in Medicine & Biology, 51(23), p.6099. https://doi.org/10.1088/0031-9155/51/23/011 PMid:17110773

26. Studenski MT, Xiao Y. Proton therapy dosimetry using positron emission tomography. World J Radiol. 2010,4;2(4):135. https://doi.org/10.4329/wjr.v2.i4.135 PMid:21160579 PMCid:PMC2998812

How to Cite This Article:

Khoshhal A R, Esmaili Torshabi A, Babamohammadi S. Investigation of the Produced Positrons and Their Dose Deposition at Bone and Soft Tissue Organs at Proton Therapy: A Simulation Study. J Adv Med Biomed Res 2024; 32 (155) :405-414

Download citation:
BibTeX | RIS | EndNote | Medlars | ProCite | Reference Manager | RefWorks

Send citation to:
Mendeley Zotero RefWorks